DOI 10.31891/2307-5732-2024-333-2-44
UDC 004.932

KRYVENKO SERGII
National Aerospace University – KhAI
https://orcid.org/0000-0001-6027-5442
e-mail: s.kryvevnko@khai.edu
LUKIN VLADIMIR
National Aerospace University – KhAI
https://orcid.org/0000-0002-1443-9685
e-mail: v.lukin@khai.edu

PECULIARITIES OF NOISY IMAGE LOSSY COMPRESSION

This paper deals with lossy compression applied to grayscale noisy images using several coders. The case of additive white Gaussian noise is considered as the first step in studying the problem. A special attention is paid to quite new coders AVIF and HEIF for which, to the best of our knowledge, lossy compression of noisy images of different complexity has not been thoroughly considered yet. It is shown that optimal operation point is possible for all coders under certain conditions according to different quality metrics including conventional peak signal-to-noise ratio and visual quality metrics such as PSNR-HVS-M and MS-SSIM. The compression parameters (metrics) in optimal operation point significantly depend on image complexity and noise intensity where the existence of optimal operation point is more probable for simple structure images and/or intensive noise. Comparison of metric values in optimal operation point for the considered coders shows that slightly better characteristics are provided by better portable graphics (BPG) and advanced discrete cosine transform (ADCT) coders. The results for JPEG are significantly worse. The AVIF and HEIF encoders provide similar results and they outperform JPEG significantly. Optimal operation point for all studied coders is observed more rarely for visual quality metrics than for peak signal-to-noise ratio. General tendencies concerning dependence of optimal compression parameters on noise intensity are presented. It is shown that compression ratio in optimal operation point is often larger than 20 and can be as large as 60. The problem with AVIF and HEIF is that it is currently unclear how to choose quality factor for them to carry out lossy image compression in the neighborhood of the corresponding optimal operation point. Meanwhile, there is the tendency to optimal quality factor reduction if intensity of additive white Gaussian noise increases. The directions of further research are discussed.

Keywords: lossy image compression, noise, optimal operation point, performance comparison

КРИВЕНКО СЕРГІЙ
Національний аерокосмічний університет ім. М.Є. Жуковського "ХАІ"
ЛУКІН ВОЛОДИМИР
Національний аерокосмічний університет ім. М.Є. Жуковського "ХАІ"

ОСОБЛИВОСТІ СТИСНЕННЯ З ВТРАТАМИ ЗОБРАЖЕНЬ ІЗ ШУМОМ

У цій статті розглядається стиснення з втратами, що застосоване до зображень із шумами, за допомогою кількох кодерів. Показано, що оптимальна робоча точка можлива для всіх кодерів за певних умов відповідно до різних показників якості. Параметри стиснення в оптимальній робочій точці істотно залежать від складності зображення та інтенсивності шуму. Порівняння показує, що дещо кращі характеристики забезпечують кодери BPG та ADCT. Наведено загальні тенденції щодо залежності оптимальних параметрів компресії від інтенсивності шуму. Обговорено напрямки подальших досліджень.

Ключові слова: стиснення зображень із втратами, шум, оптимальна робоча точка, порівняння характеристик

Problem overview

A general number of images acquired nowadays by different sensors rapidly increases where images are obtained by customer devices [1], medical equipment [2], from satellite and drones [3, 4] and so on. Image mean size increases as well. This results in problems of image transfer, processing, and storage [5, 6]. Hence, image compression is an operation typical for many modern applications [5–7]. Lossless and lossy compression are two options having their own advantages and drawbacks. Lossless compression does not introduce distortions but the compression ratio (CR) for this class of methods is usually is often too small and cannot be varied [8]. This explains popularity of lossy compression represented by a wide variety of the corresponding techniques [7, 8]. Lossy compression produces distorted images but it is often possible to control distortions and provide an appropriate trade-off between the attained CR and compressed image quality. Recall that quality can be characterized directly by some standard or visual quality metrics [9] or, indirectly, by the influence of lossy compression in terms of compressed image, object recognition, and so on [9, 10].

In most applications of lossy compression, an image subject to compression is supposed noise-free or, at least, possible noise presence is ignored. Meanwhile, there are applications for which an acquired image is noisy [11–13]. Then, approaches to design and analysis of lossy compression of noisy images differ from those ones typical for lossy compression of noise-free images [14, 15]. This deals with specific noise filtering effect that takes place in lossy compression of noisy images as well as possible presence of optimal operation point (OOP) [14–16]. OOP is such a value of a parameter that controls compression (PCC) for a given coder for which compressed image is “the closest” to the corresponding true (noise-free) image according to a chosen quality metric and closer than the corresponding noisy (original, uncompressed) image. Here it is worth noting that OOP existence depends on image properties, noise type and intensity, a coder and a metric used. If OOP for a given noisy image and coder exists, then it is reasonable to compress it in OOP; otherwise, other recommendations on PCC setting can be taken into account [17].

Possible existence of OOP has been demonstrated for JPEG and JPEG2000 [18] in [15], for AGU [19], ADCT [20] and BPG [21] coders in [15], [16], and [17], respectively. Note that PCCs for these coders are different: quality factor (QF) for JPEG, bits per pixel (BPP) for JPEG2000, quantization step (QS) for the AGU and ADCT coder, parameter Q for the BPG encoder. This leads to the necessity to carry out special studies for designing the procedures of PCC setting in OOP (if it exists) for each coder depending on noise intensity. For AGU, ADCT, and BPG encoders, these procedures are quite simple under assumption that noise characteristics are a priori known or have been accurately estimated in advance [22, 23]. Meanwhile, for JPEG and JPEG2000, determination of QF and BPP in OOP requires iterative procedures with multiple compression and decompression.

Recently, new encoders, namely AVIF [24] and HEIF [25], have been designed and shown to be rather efficient. Meanwhile, to the best of our knowledge, the studies concerning application of these encoders to compression of noisy images have not been carried out. Thus, t**he paper goal** is to check whether or not OOP is possible in lossy compression of noisy images by AVIF and HEIF. If yes, then we would like to compare the performance characteristics in OOP for these two encoders to data for other known encoders. As a starting point of such studies, we consider the case of grayscale images corrupted by white additive Gaussian noise (AWGN).

Analysis of recent sources

It is known that lossy image compression techniques are usually characterized by rate-distortion curves (RDCs), i.e. dependencies of some parameter (metric) on PCC used for a given coder. Such dependences are usually monotonous functions. The examples are dependences of peak signal-to-noise ratio (PSNR) on QF for JPEG that are monotonously increasing functions [26] or dependences of PSNR on QS or CR for AGU [27] that are monotonously decreasing ones. This monotonicity shows the main tendency that quality of a compressed image becomes worse according to any metric if CR increases (BPP decreases). Then, it becomes easy to compare the coders' performance by fixing CR for a given image and comparing the values of a considered metric. An example of RDCs (dependence of visual quality metric PSNR-HVS-M (https://ponomarenko.info/psnrhvsm.htm) on CR for five different coders for a 512×512 pixel fragment of dental medical image is presented in Fig. 1. As one can see, the ADCT, BPG and modified AGU encoders provide significantly better quality of compressed image for a wide range of CR values according to the visual quality metric PSNR-HVS-M expressed in dB (larger values correspond to a better quality). Taking into account that visually noticeable distortions start to appear when PSNR-HVS-M is smaller than 40 dB, it is possible provide visually lossless compression for the ADCT, BPG and modified AGU encoders for CR up to 14 whilst the distortions become visible for JPEG and JPEG2000 is CR exceeds 10.

The situation is more complex in lossy compression of noisy images. Then, one might analyze not only traditional RDCs (as in Fig. 1) but also dependences for metrics calculated between compressed and noise-free images. In practice, it is impossible to obtain such dependences since noise-free image is absent, but it is possible to obtain them for simulated data when noise is artificially added to a noise-free image and then the obtained noisy image is compressed in a lossy manner [15–17].

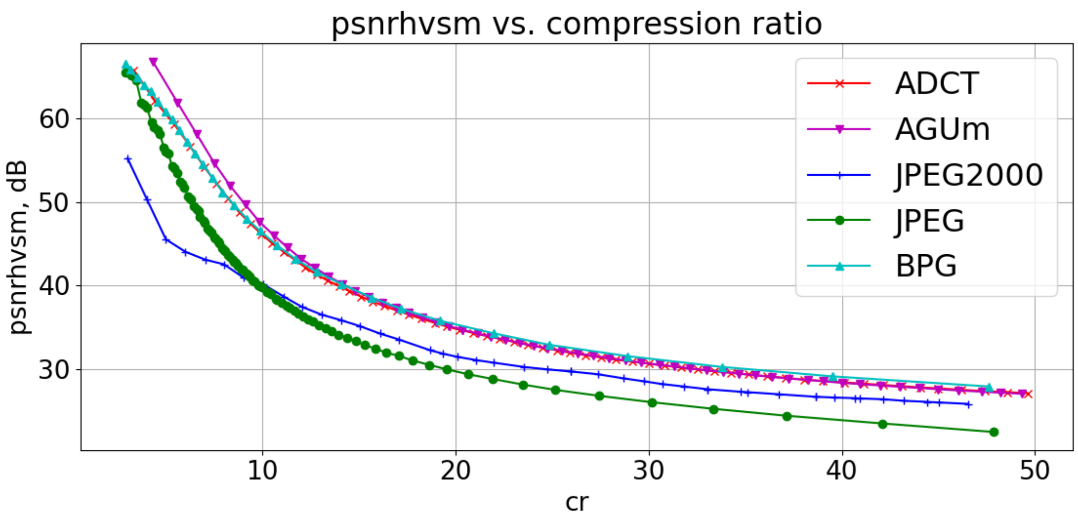

Fig. 1. RDCs for five encoders for a 512×512 pixel fragment of dental medical image

Fig. 2 presents such dependences for the conventional grayscale test image Peppers corrupted by AWGN with zero mean and variance σ^2 equal to 100 (all noise-free test images considered below are 8-bit). A problem was to present all dependences together since PCCs are different for different coders. Because of this, the horizontal axis is used for the following PCCs: QF for JPEG, AVIF, and HEIF where smaller values correspond to a larger CR; QS and the parameter Q for the ADCT and BPG encoders, respectively, where larger QS and Q relate to a larger CR. As one can see, the main observations are the following:

1) PSNR is about 28 dB (approximately equal to 10lg(2552/σ2) for small CR (that corresponds to small QS and Q and larger QF);

2) PSNR is larger than 28 dB for certain interval of PCC values where maxima are observed for QS≈41 for ADCT, Q≈35 for BPG, QF≈15 for JPEG, QF≈25 for HEIF, and QF≈31 for AVIF coders; this means that OOPs according to PSNRtc exist for all five encoders;
3) PSNRtc values in OOP are different; PSNRtc is the smallest for JPEG, and it is the largest for the BPG encoder;
4) PSNRtc values for the encoders HEIF and AVIF in OOP are almost the same; it is also worth noting that $PSNR_{tc}$ in neighbor QF values for these two coders are the same.

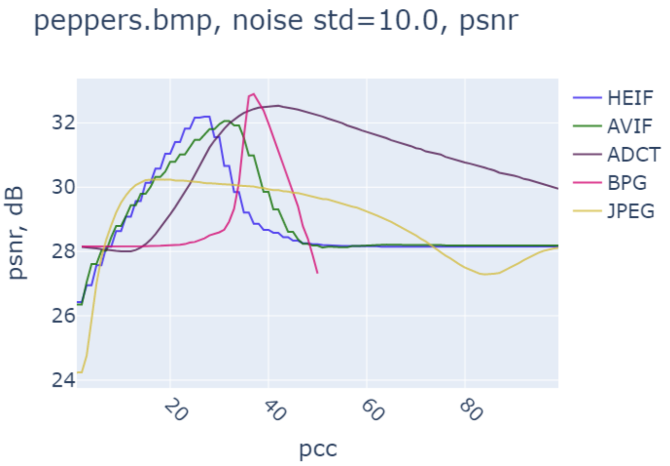

Fig. 2. Dependences $PSNR_{tc}$ vs PCC for the test image Peppers corrupted by AWGN with variance equal to 100 compressed by five considered coders

The dependences can be compared in another way – using CR as horizontal axis. The obtained data are represented in Fig. 3. As one can see, compression in OOP (with providing the largest possible $PSNR_{tc}$) produces sufficiently different values of CR: about 20 for JPEG, about 24 for the ADCT coder, and larger than 40 for the HEIF, AVIF, and BPG encoders. Thus, although ADCT coder provides slightly larger $PSNR_{OOP}$ ($PSNR_{tc}$ in OOP), it produces significantly smaller CR_{OOP}(CR in OOP). Because of this, the modern encoders BPG, AVIF and HEIF can be preferable.

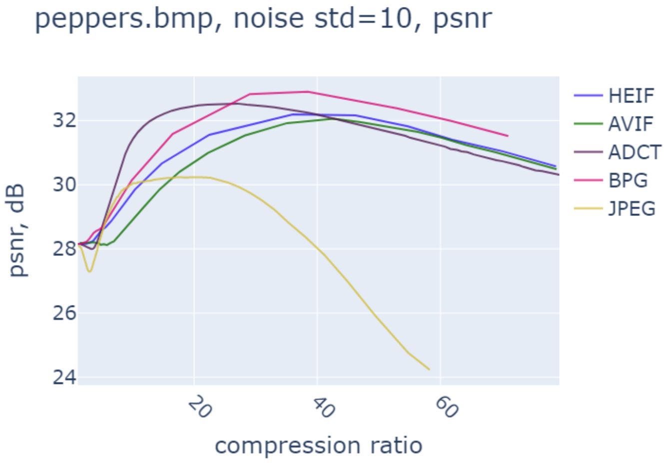

Fig. 3. Dependences $PSNR_{tc}$ vs CR for the test image Peppers corrupted by AWGN with variance equal to 100 compressed by five considered coders

It might also happen that OOP is absent. Fig. 4 shows an example of the corresponding dependences for the test image Baboon (known to be highly textural or having complex structure) corrupted by AWGN with σ^2=100. Formally, there is no OOP for all encoders (although there are local maxima for the ADCT and BPG encoders in which $PSNR_{tc}$ are slightly smaller than $PSNR_{tc}$(CR→1). JPEG produces the smallest $PSNR_{tc}$ in all the considered range of CR. The BPG and ADCT encoders provide better $PSNR_{tc}$ than AVIF and HEIF encoders for CR≈6. However, starting from CR≈20, there is practically no difference for the BPG, ADCT, AVIF, and HEIF encoders.

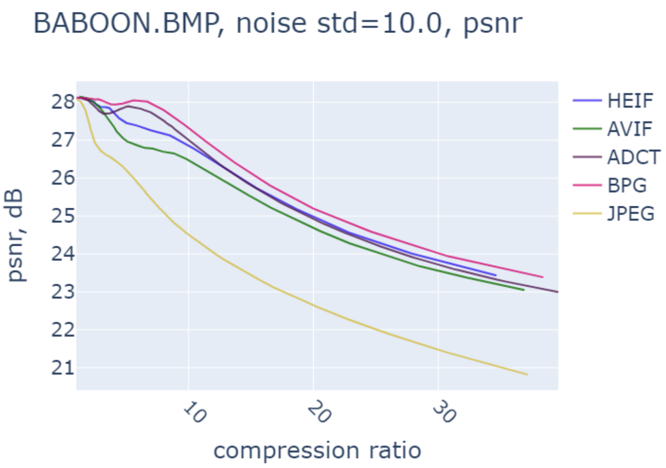

Fig. 4. Dependences $PSNR_{tc}$ vs CR for the test image Baboon corrupted by AWGN with variance equal to 100 compressed by five considered coders

Having explained the phenomenon of OOP and its possible existence or absence, we would like to recall the basic tendencies known from the earlier obtained results. First, OOP can exist not only according to traditional metric such as PSNR but also according to visual quality metrics [17] such as aforementioned PSNR-HVS-M or MS-SSIM [28]. Second, if the noise variance increases, PCC corresponding to OOP shifts towards its value that corresponds to a larger CR (i.e., a larger Q or QS and smaller QF). Third, if noise variance increases, probability that OOP exists increases as well [16, 29]. Fourth, PCC_{OOP} for conventional and visual quality metrics are almost the same. These properties will be checked in the next section of this paper.

Presentation of the main material

Let us start our analysis from considering the data for the visual quality metric MS-SSIM for which it is known that its maximal possible value is equal to unity and a larger MS-SSIM relates to better visual quality. Dependences of $MS\text{-}SSIM_{tc}$ on CR are given in Fig. 5 for the test image Pepper. The first observation is that OOP exists for all five considered coders where the largest $MS\text{-}SSIM_{tc}$ is again observed for the BPG encoder and the worst

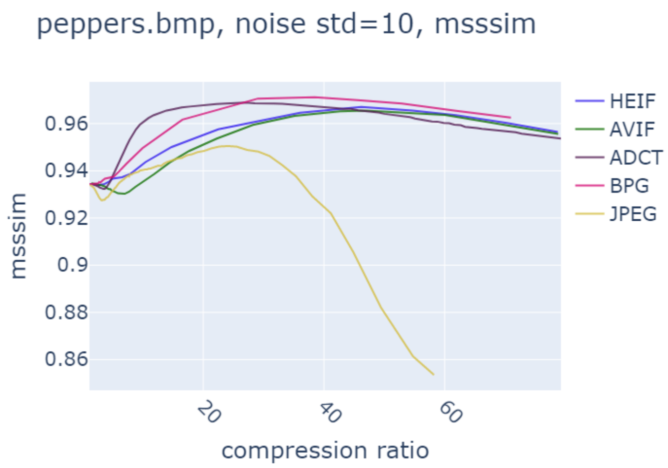

Fig. 5. Dependences MS-SSIM$_{tc}$ vs CR for the test image Peppers corrupted by AWGN with variance equal to 100 compressed by five considered coders

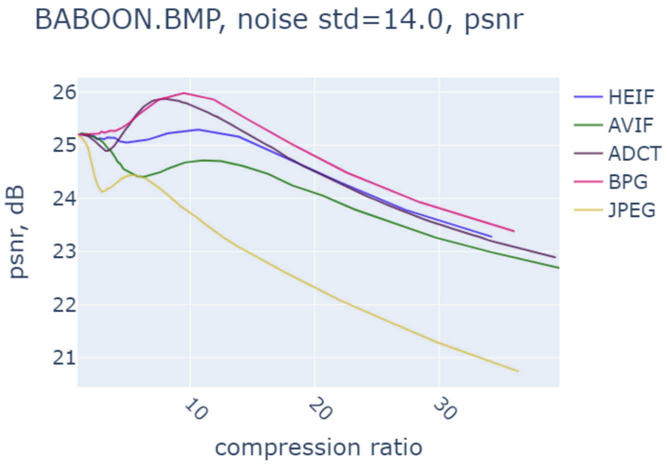

Fig. 6. Dependences PSNR$_{tc}$ vs CR for the test image Baboon corrupted by AWGN with variance equal to 196 compressed by five considered coders

takes place for JPEG. Compression in OOP (according to MS-SSIM$_{tc}$) produces CR about 23 for JPEG, about 25 for the ADCT coder, and larger than 40 for the HEIF, AVIF, and BPG encoders. This example confirms that OOPs according to different metrics are almost the same.

Consider now the plots for the test image Baboon corrupted by AWGN with $\sigma^2=196$ (Fig. 6). The main observations are the following. First, for three coders (BPG, ADCT, HEIF), OOPs are present (although OOPs were absent for $\sigma^2=100$, see the plots in Fig. 4). The results are again the best for the BPG encoder and the worst for JPEG. Second, positions of maxima have shifted towards larger CR values.

To prove the second property, we have obtained dependences PSNR$_{tc}$ vs CR for the test image Peppers corrupted by AWGN with variances 25 and 196. They are shown in Figures 7 and 8, respectively. There is no OOP for JPEG for $\sigma^2=25$ (Fig. 7) although it is observed for $\sigma^2=100$ (Fig. 3) and $\sigma^2=100$ (Fig. 8). Formally, there is no OOP for AVIF for $\sigma^2=25$ (Fig. 7) although it is takes place for $\sigma^2=100$ (Fig. 3) and $\sigma^2=100$ (Fig. 8). Thus, OOP existence is more probable for higher noise intensity. In addition, OOP happens for larger CR in noise is more intensive – for the encoder HEIF, CR$_{OOP}\approx13$ for $\sigma^2=25$ (Fig. 7), approximately 35 for $\sigma^2=100$ (Fig. 3), and approximately 45 for $\sigma^2=196$ (Fig. 8).

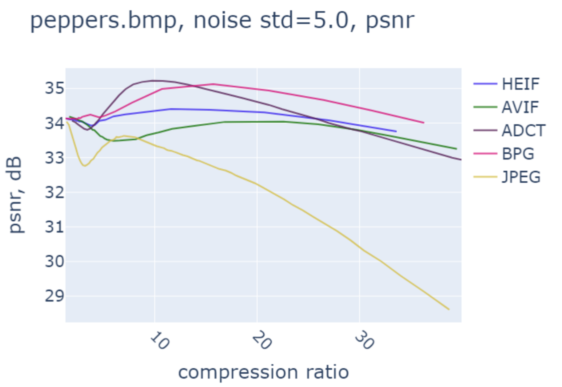

Fig. 7. Dependences PSNR$_{tc}$ vs CR for the test image Peppers corrupted by AWGN with variance equal to 25 compressed by five considered coders

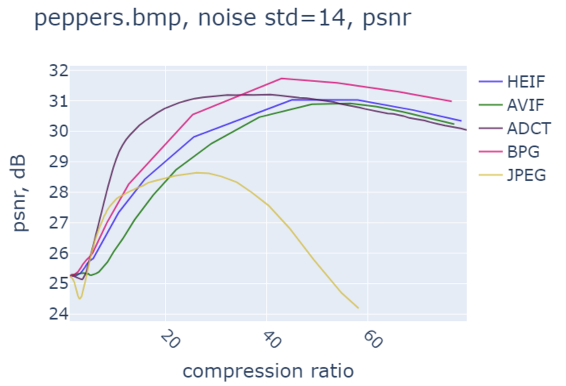

Fig. 8. Dependences PSNR$_{tc}$ vs CR for the test image Peppers corrupted by AWGN with variance equal to 196 compressed by five considered coders

Finally, let us also present the plots MS-SSIM$_{tc}$ vs CR for the test image Peppers corrupted by AWGN with variance equal to 196 (Fig. 9). As seen, OOPs take place for all five encoders where the best results are provided by the BPG encoder. The values of CR$_{OOP}$ are practically the same as for the PSNR metric (Fig. 8) for the corresponding coders. Meanwhile, the values of CR$_{OOP}$ are larger than for the same test image but the smaller noise variance (compare to data in Fig. 5.

Therefore, we can state that the properties earlier observed for JPEG, ADCT, and BPG encoders take place for AVIF and HEIF as well. The possibility of OOP existence for them according to different metrics is clearly demonstrated. The performance characteristics are significantly better than for JPEG and are quite similar to those ones observed for the BPG and ADCT encoders although, in aggregate, the results for the BPG encoder are slightly better.

Meanwhile, there are several questions valuable for practice that have left not answered. The main among them is how to determine the OOP (QF_{OOP}) for a given image and noise variance. Second, we wonder do the discovered properties hold for other than optical (e.g., medical or remote sensing) types of images. Third, a question is whether or not it is possible to predict OOP existence before compression.

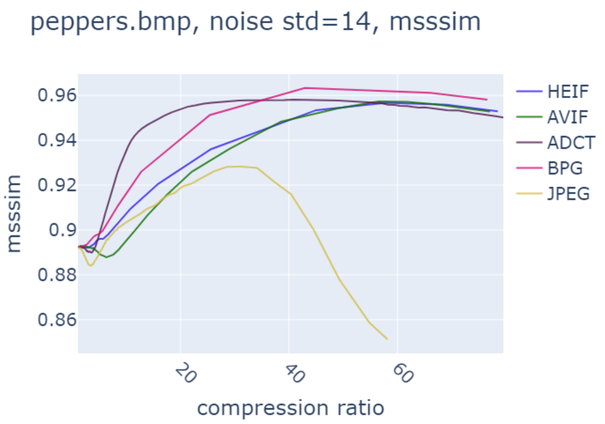

Fig. 9. Dependences MS-SSIM$_{tc}$ vs CR for the test image Peppers corrupted by AWGN with variance equal to 196 compressed by five considered coders

Conclusions

We have considered the task of lossy compression of grayscale images corrupted by AWGN by five coders including such modern ones as AVIF and HEIF. It is shown that the effects earlier found for other coders such as JPEG, ADCT, and BPG (in particular, possible OOP existence) take place for AVIF and HEIF as well. The results for AVIF and HEIF are of about the same level as for ADCT, slightly worse than for the BPG encoder, but significantly better than for JPEG. The OOP possible existence is shown for two optical test images of different complexity according to both conventional and visual quality metrics (especially, for the cases of intensive noise). It is stated that the studies have to be continued for other types of the images and noise. The main practical issue is to design a procedure to determine and set QF_{OOP}.

References

1. Deever A. Digital camera image formation: processing and storage / A. Deever, M. Kumar, B. Pillman // Digital Image Forensics / H. T. Sencar, N. Memon. — New York, NY : Springer New York, 2013. — P. 45–77.

2. Gulo C. A. S. J. Techniques of medical image processing and analysis accelerated by high-performance computing: a systematic literature review / C. A. S. J. Gulo, A. C. Sementille, J. M. R. S. Tavares // Journal of Real-Time Image Processing. — 2019. — Vol. 16, No. 6. — P. 1891–1908.

3. Zhang Z. A review on unmanned aerial vehicle remote sensing: platforms, sensors, data processing methods, and applications / Z. Zhang, L. Zhu // Drones. — 2023. — Vol. 7, No. 6. — P. 398.

4. Luo L. Airborne and spaceborne remote sensing for archaeological and cultural heritage applications: a review of the century (1907–2017) / L. Luo, X. Wang, H. Guo, [et al.] // Remote Sensing of Environment. — 2019. — Vol. 232. — P. 111280.

5. Shelke S. K. Study of end to end image processing system including image de-noising, image compression & image security / S. K. Shelke, S. K. Sinha, G. S. Patel // Wireless Personal Communications. — 2021. — Vol. 121, No. 1. — P. 209–220.

6. Pan S. Research on mass image data storage method for data center / S. Pan, J. Jiang, H. Qiu, [et al.] // 3D Imaging—Multidimensional Signal Processing and Deep Learning / S. Patnaik, R. Kountchev, Y. Tai, R. Kountcheva. — Singapore : Springer Nature Singapore, 2023. — P. 69–75.

7. Fu C. Remote sensing image compression based on the multiple prior information / C. Fu, B. Du // Remote Sensing. — 2023. — Vol. 15, No. 8. — P. 2211.

8. Hussain A. J. Image compression techniques: a survey in lossless and lossy algorithms / A. J. Hussain, A. Al-Fayadh, N. Radi // Neurocomputing. — 2018. — Vol. 300. — P. 44–69.

9. Li F. A fast method for visual quality prediction and providing in image lossy compression by spiht / F. Li, S. Krivenko, V. Lukin // Integrated Computer Technologies in Mechanical Engineering - 2020 / M. Nechyporuk, V. Pavlikov, D. Kritskiy. — Cham : Springer International Publishing, 2021. — P. 17–29.

10. Radosavljević M. Lossy compression of multispectral satellite images with application to crop thematic mapping: a hevc comparative study / M. Radosavljević, B. Brkljač, P. Lugonja, [et al.] // Remote Sensing. — 2020. — Vol. 12, No. 10. — P. 1590.

11. Ponomarenko N. N. LOSSY and visually lossless compression of single-look sar images / N. N. Ponomarenko, V. V. Lukin, R. A. Kozhemiakin, [et al.] // Telecommunications and Radio Engineering. — 2013. — Vol. 72, No. 8. — P. 711–729.

12. Reddy P. L. Multispectral image denoising methods: a literature review / P. L. Reddy, S. Pawar // Materials Today: Proceedings. — 2020. — Vol. 33. — P. 4666–4670.

13. Mohd Sagheer S. V. A review on medical image denoising algorithms / S. V. Mohd Sagheer, S. N. George // Biomedical Signal Processing and Control. — 2020. — Vol. 61. — P. 102036.

14. Al-Shaykh O. K. Lossy compression of noisy images / O. K. Al-Shaykh, R. M. Mersereau // IEEE Transactions on Image Processing. — 1998. — Vol. 7, No. 12. — P. 1641–1652.

15. Ponomarenko N. Lossy compression of images with additive noise / N. Ponomarenko, V. Lukin, M. Zriakhov, [et al.] // Advanced Concepts for Intelligent Vision Systems / J. Blanc-Talon, W. Philips, D. Popescu, P. Scheunders. — Berlin, Heidelberg : Springer Berlin Heidelberg, 2005. — P. 381–386.

16. Zemliachenko A. N. Lossy compression of noisy remote sensing images with prediction of optimal operation point existence and parameters / A. N. Zemliachenko, S. K. Abramov, V. V. Lukin, [et al.] // Journal of Applied Remote Sensing. — 2015. — Vol. 9, No. 1. — P. 095066.

17. Lukin V. Compression of noisy images taking into account visual quality: a comprehensive study / V. Lukin, B. Kovalenko, S. Kryvenko, [et al.] // Research Developments in Science and Technology Vol. 8. — 2022. — P. 89–109.

18. Pancholi B. Tutorial review on existing image compression techniques / B. Pancholi, R. Shah, M. Modi // Int. J. Eng. Comput. Sci. — 2014. — Vol. 3, No. 8. — P. 7882–7889.

19. Ponomarenko N. DCT based high quality image compression / N. Ponomarenko, V. Lukin, K. Egiazarian, J. Astola // Image Analysis / H. Kalviainen, J. Parkkinen, A. Kaarna. — Berlin, Heidelberg : Springer Berlin Heidelberg, 2005. — P. 1177–1185.

20. Ponomarenko N. N. High-quality dct-based image compression using partition schemes / N. N. Ponomarenko, K. O. Egiazarian, V. V. Lukin, J. T. Astola // IEEE Signal Processing Letters. — 2007. — Vol. 14, No. 2. — P. 105–108.

21. BPG image format. Online access: https://bellard.org/bpg/

22. Vozel B. Noise identification and estimation of its statistical parameters by using unsupervised variational classification / B. Vozel, K. Chehdi, L. Klaine, [et al.]. — Toulouse, France : IEEE, 2006.

23. Abramova V. Blind evaluation of noise characteristics in multichannel images / V. Abramova, S. Abramov, K. Abramov, B. Vozel // Information Technologies in the Design of Aerospace Engineering / M. Nechyporuk, V. Pavlikov, D. Krytskyi. — Cham : Springer Nature Switzerland, 2024. — P. 209–229.

24. Rahman Md. A. The impact of state-of-the-art techniques for lossless still image compression / Md. A. Rahman, M. Hamada, J. Shin // Electronics. — 2021. — Vol. 10, No. 3. — P. 360.

25. Lainema J. HEVC still image coding and high efficiency image file format / J. Lainema, M. M. Hannuksela, V. K. M. Vadakital, E. B. Aksu. — Phoenix, AZ, USA : IEEE, 2016.

26. Bondžulić B. Efficient prediction of the first just noticeable difference point for jpeg compressed images / B. Bondžulić, N. Stojanović, V. Petrović, [et al.] // Acta Polytechnica Hungarica. — 2021. — Vol. 18, No. 8. — P. 201–220.

27. Krivenko S. S. SMART lossy compression of images based on distortion prediction / S. S. Krivenko, O. Krylova, E. Bataeva, V. V. Lukin // Telecommunications and Radio Engineering. — 2018. — Vol. 77, No. 17. — P. 1535–1554.

28. Wang Z. Multiscale structural similarity for image quality assessment / Z. Wang, E. P. Simoncelli, A. C. Bovik. — Pacific Grove, CA, USA : IEEE, 2003.

29. Kovalenko B. BPG-based automatic lossy compression of noisy images with the prediction of an optimal operation existence and its parameters / B. Kovalenko, V. Lukin, S. Kryvenko, [et al.] // Applied Sciences. — 2022. — Vol. 12, No. 15. — P. 7555.